ISSN 0018-151X, High Temperature, 2007, Vol. 45, No. 2, pp. 137–142. © Pleiades Publishing, Ltd., 2007.
Original Russian Text © E.N. Vasil'ev, D.A. Nesterov, 2007, published in Teplofizika Vysokikh Temperatur, Vol. 45, No. 2, 2007, pp. 165–170.

PLASMA INVESTIGATIONS

Numerical Simulation of Interaction between Arc Discharge and Transverse Magnetic Field

E. N. Vasil'ev and D. A. Nesterov

Institute of Computational Modeling, Siberian Division, Russian Academy of Sciences, Krasnoyarsk, 660036 Russia

Received January 10, 2006

Abstract—An unsteady-state three-dimensional numerical model of radiation magnetogasdynamics is used to calculate the structure of an arc discharge which interacts with an external transverse magnetic field and transverse gas flow. The velocity field and the distribution of gas temperature obtained as a result of calculations agree with experimental data. The difference between the calculated and measured values of temperature in the discharge column is approximately 5%.

PACS numbers: 52.30.-q, 52.30.Cv, 52.80.Mg

DOI: 10.1134/S0018151X07020010

INTRODUCTION

The high capacity of present-day computer equipment defines ever more extensive uses of three-dimensional numerical models for describing high-temperature gasdynamic flows which are characterized by complexity and diversity of processes occurring in them. In particular, a steady-state three-dimensional model was used to obtain calculation results for electric-arc argon plasma, which fairly well agree with the experimental data [1, 2]. The present study is a continuation of investigations involving the use of two-dimensional [3, 4] and three-dimensional [5, 6] computational models of unsteady-state nonuniform flows of electrically conducting gas interacting with external magnetic field under conditions of radiative-convective heat transfer. In [3, 6], we studied the dynamics of self-sustaining current layers. In [4], the results are given of simulation of the structure of a high-current discharge in the channel of a railgun accelerator for the experimental conditions of [7]. No measurements of local values of physical parameters were performed in the experiments of [7] and, therefore, no quantitative comparison of theoretical and experimental results could be made; however, the simulation made it possible to investigate the dynamics of the process and identify the physical mechanisms which caused the formation of the experimentally observed unsteady-state and irregular structure of discharge.

In the present study, we use a three-dimensional numerical model to investigate the interaction between an arc discharge (subjected to transverse blowing over) and external magnetic field and to compare the calculation results with the experimental data of Sebald [8].

FORMULATION OF THE PROBLEM

The scheme of the process being investigated is given in Fig. 1. The column of arc discharge is blown over by a flow of nitrogen at atmospheric pressure in a channel of constant cross section. The channel height (spacing between the electrodes) is 5 cm and the channel width 6 cm. The current flowing in the arc was varied in the experiments from 15 to 25 A, the magnetic field induction B was varied from 1.6×10^{-3} to 1.4×10^{-3} T, the velocity of blowing-over was constant and equal to 0.8 m/s. The temperature distribution was measured in the experiments (Fig. 2), and the velocity field for the mean cross section of the channel was determined.

The following basic assumptions were made in the numerical simulation of the process:

—the thermal interaction between the arc and the electrodes is described by the mechanism of heat conduction alone, no other processes are considered on the electrodes and in the electrode regions, the temperature of electrodes and gas flow at the channel inlet is taken to be constant;

—it is assumed that the radiation leaving the discharge region is fully absorbed by the channel walls, and that the self-radiation of the walls is negligible due to their low temperature; and

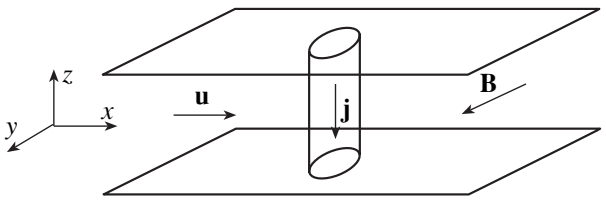

Fig. 1. The scheme of the process in the channel.

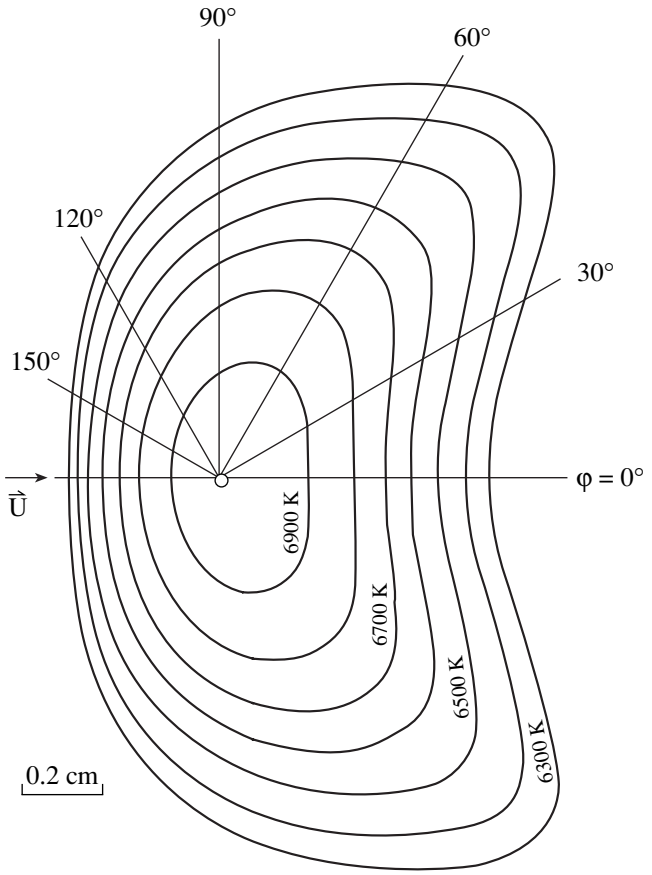

Fig. 2. The distribution of gas temperature in the mean horizontal cross section of the arc, experimentally obtained in [8].

—the impact of induced magnetic field and of the associated pinch effect was ignored; the value of this field, determined by the formula for an infinite straight conductor $B_{\text{ind}} = \mu_0 I/2\pi r$ at current strength $I = 20$ A and characteristic radius of discharge $r = 1$ cm, is 4×10^{-4} T, which is low compared to external magnetic field.

The computational model of the process is based on the solution of gasdynamic and electrodynamic equations and of the equation of radiative transfer. The motion of gas is described using a set of Euler equations,

$$\frac{\partial \mathbf{U}}{\partial t} + \frac{\partial \mathbf{E}}{\partial x} + \frac{\partial \mathbf{F}}{\partial y} + \frac{\partial \mathbf{G}}{\partial z} = \mathbf{S}, \tag{1}$$

$$\mathbf{U} = \begin{bmatrix} \rho \\ \rho u \\ \rho v \\ \rho w \\ E_t \end{bmatrix}, \quad \mathbf{E} = \begin{bmatrix} \rho u \\ \rho u^2 + p \\ \rho uv \\ \rho uw \\ (E_t + p)u + q_x \end{bmatrix},$$

$$\mathbf{F} = \begin{bmatrix} \rho v \\ \rho vu \\ \rho v^2 + p \\ \rho vw \\ (E_t + p)v + q_y \end{bmatrix}, \tag{2}$$

$$\mathbf{G} = \begin{bmatrix} \rho w \\ \rho wu \\ \rho wv \\ \rho w^2 + p \\ (E_t + p)w + q_z \end{bmatrix}, \quad \mathbf{S} = \begin{bmatrix} 0 \\ f_x \\ f_y \\ f_z \\ Q \end{bmatrix},$$

$$E_t = \rho\left(\frac{u^2 + v^2 + w^2}{2} + e\right), \tag{3}$$

$$Q = Q_J - Q_R + f_x u + f_y v + f_z w,$$

$$q_x = -\lambda\frac{\partial T}{\partial x}, \quad q_y = -\lambda\frac{\partial T}{\partial y}, \quad q_z = -\lambda\frac{\partial T}{\partial z}, \tag{4}$$

$$p = R\rho T, \quad e = RT/(\gamma - 1), \tag{5}$$

where t is the time; ρ, p, and T denote the gas density, pressure, and temperature, respectively; u, v, and w are components of the gas velocity vector $\mathbf{v}$; E_t is the total energy per unit volume of gas; e is the internal energy per unit mass of gas; f_x, f_y, and f_z are components of the vector of force $\mathbf{f}$ acting on the gas along the x, y, and z coordinate axes, respectively; Q_J is the volumetric power of Joule dissipation, and Q_R is the power of radiation sources and sinks of energy; λ is the thermal conductivity coefficient of gas; R is the individual gas constant; and γ is the adiabatic exponent.

The scalar function of electric field potential φ, which satisfies the equation

$$-\nabla\varphi = \mathbf{E}^e \tag{6}$$

is used to describe the electromagnetic interaction. In view of the validity within the computational domain of Ohm's law $\mathbf{j} = \sigma(\mathbf{E}^e + \mathbf{v} \times \mathbf{B})$, of relation $\text{div}\mathbf{j} = 0$ following from the Maxwell equations, and of formula (6), we derive an inhomogeneous elliptic equation with variable coefficients,

$$\text{div}(\sigma\nabla\varphi) = \text{div}(\sigma \cdot (\mathbf{v} \times \mathbf{B})). \tag{7}$$

In these relations, $\mathbf{E}^e$ is the electric field intensity, $\mathbf{j}$ is the current density, and σ is the electrical conductivity of gas. In spite of the fact that the discharge column is by and large stationary, the induced electric field $\mathbf{v} \times \mathbf{B}$ is included in the model, because it was experimentally found that the gas within the discharge performs vortex motion. The solution of Eq. (7) enables one to find the potential distribution $\varphi(x, y, z)$, by which the distributions $\mathbf{E}^e(x, y, z)$ are determined from (6) and $\mathbf{j}(x, y, z)$

using Ohm's law, as well as Joule dissipation $Q_J = j^2/\sigma$ and Lorentz force $\mathbf{f} = \mathbf{j} \times \mathbf{B}$.

The following equations are solved in order to calculate the volumetric variation of energy Q_R due to radiative transfer:

$$\mathbf{\Omega} \cdot \mathrm{grad}(I_\nu) = k_\nu(I_{\nu p} - I_\nu), \quad (8)$$

$$\mathbf{W} = \int_0^\infty d\nu \int \mathbf{a} I_\nu d\Omega, \quad (9)$$

$$Q_R = \mathrm{div}(\mathbf{W}), \quad (10)$$

where I_ν is the intensity of energy of radiation of frequency ν, $I_{\nu p} = 2h\nu^3/[c^2(\exp\{h\nu/(kT)\} - 1)]$ is the intensity of equilibrium radiation, $k_\nu(\nu, T, p)$ is the radiation absorption coefficient, $\mathbf{a}$ is the unit vector which defines the direction of radiation for angle $d\Omega$, and $\mathbf{W}$ is the vector of radiation energy flux.

The transfer equation (8) is a one-dimensional ordinary differential equation which describes the variation of radiation intensity along the preassigned direction. In a three-dimensional case, each point of the difference grid is connected with neighboring nodes in six directions. A multigroup approximation is used for solving the transfer equation, where the entire frequency spectrum is divided into groups (in this calculation, 560 groups), with the absorption coefficient in each group taken to be constant. At each time step, the differential equation is integrated numerically for all directions and spectral groups. The calculation of loss of energy due to radiation is most time-consuming; therefore, the equations of radiative transfer were solved only for the arc and immediate neighborhood.

Also employed in the calculations was a simplified radiation model, i.e., a volume radiator approximation, in which the radiative energy loss is determined by the emissivity factors of hemispherical radiating volume $\varepsilon(T, p, \delta)$,

$$Q_R = 4\sigma_R \varepsilon(T, p, \delta) T^4/\delta. \quad (11)$$

Here, σ_R is the Stefan–Boltzmann constant, and δ is the characteristic size of radiating volume of gas. The presence of factor 4 in formula (11) is associated with the conversion of Q_R upon transition from the hemispherical to cubic volume. Formula (11) describes the process of radiative heat transfer disregarding the spectral and angular characteristics; owing to the use of this formula, the calculation of Q_R is simple to realize and does not require much computational effort.

A detailed description of computational algorithm of Eqs. (1)–(10) and the results of test calculations are given in [5].

CALCULATION RESULTS

We considered a discharge at current strength I = 19.3 A and external magnetic field induction $B = 1.5 \times 10^{-3}$ T. With these parameters, the experiment produced, for mean cross section, the temperature distribution (Fig. 2) with maximal value of 6960 K; the electric field intensity was 20 V/cm. The experimental data were further used to determine the velocity field in the discharge.

In calculations, the arc at the initial instant of time was preassigned as a cylinder with a radius of 1 cm and sine-shaped radial distribution of temperature with the maximal value at the center $T = 7 \times 10^3$ K. The initial temperature of the remaining gas and electrodes was taken to be 300 K. The transport ($\sigma(T, p)$, $\lambda(T, p)$ [9]) and radiative ($k_\nu(T, p, \nu)$, $\varepsilon(T, p, \delta)$ [10, 11]) properties of gas were introduced into the computer codes in the form of tables. The calculations were performed with different values of space steps.

The first calculation involved the use of a difference grid with equal space steps $h_x = h_y = h_z = h$ = 0.5 mm; the time step in this case was limited by the Courant criterion and amounted to $\tau \approx 0.8 \times 10^{-7}$ s. At the initial stage of interaction, the fastest variation of temperature is observed in the electrode layer of gas. Here, the high level of energy loss due to intensive heat transfer to cold electrodes results, in a fairly short period of time ($\Delta t \approx$ 0.05 ms), in the contraction of the current-conducting channel and contraction of discharge in the vicinity of the electrode surface into a microarc of a characteristic transverse dimension of approximately 2 mm. The increased current density causes a temperature increase at the arc spot on the electrode and in the zone of spreading of current (Fig. 3). In this calculation, the area of the arc spot on the electrode was 4 mm^2, the maximal value of temperature in the microarc 1.18×10^4 K, and that in the zone of spreading of current 1.47×10^4 K. At the discharge center, the temperature variation is much slower; here, the bell-shaped temperature distribution is retained, in the case of which the temperature varies monotonically from the maximal value of 6.85×10^3 K at the center to the value of slip flow temperature at the edges (Fig. 4).

Analysis of the energy balance of the arc revealed that the prevailing mechanism of energy loss in the microarc and in the zone of spreading of current is the radiation whose power may be as high as $Q_R = 2 \times 10^9$ W/m^3. The temperature in the layer of gas in direct contact with the electrode surface is largely defined by heat transfer to the electrode due to heat conduction. On the contrary, in the central part of discharge the radiation emitted in the zone of spreading of current is absorbed, $Q_R = -2 \times 10^7$ W/m^3, and the energy is extracted by heat conduction with volumetric power $Q_T = 1.5 \times 10^8$ W/m^3.

The interaction of the arc column with slip flow during time $\Delta t \approx 0.2$ ms results in the formation of two vor-

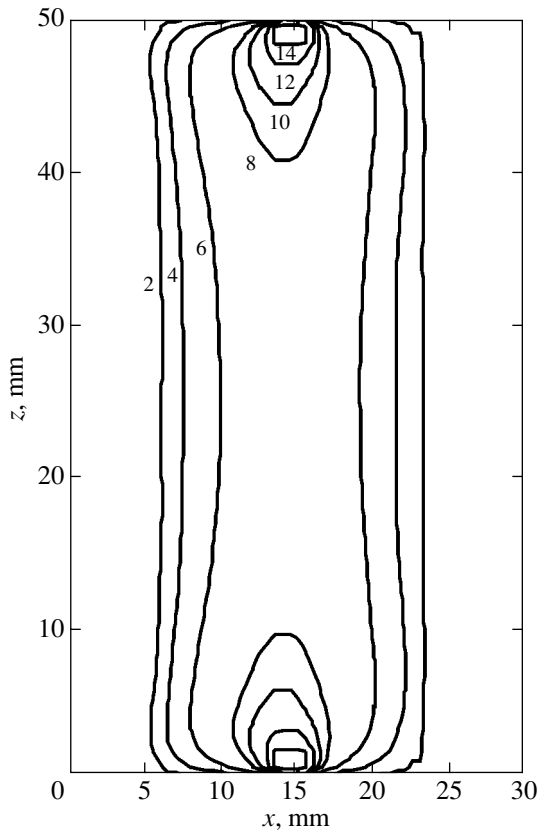

Fig. 3. The distribution of gas temperature in the vertical plane at instant of time $t = 0.7$ ms. The values of temperature on the isolines are in 10^3 K.

texes swirling in opposite directions (Fig. 4). As a result, cold gas is continuously delivered to the discharge region, while hot gas leaves that region, i.e., convective heat transfer occurs between electric-arc plasma and slip flow. The velocity of gas at the discharge center was approximately 2 m/s. In addition, the vortex flow causes a slow variation of the shape of the arc column and temperature field. This calculation was performed for a relatively short duration of the process ($\Delta t = 0.7$ ms), because the time step for the given difference grid is very small, and the calculations require much time, first of all, for solving the equation of radiation transfer. At the same time, the process at this point is still far from relaxation, and a slow variation continues both of the maximal temperature at the discharge center and of the shape of isotherms which differs significantly at this instant of time from the shape obtained experimentally. Also indicative of this is the assessment of characteristic times of formation of temperature field owing to the mechanisms of heat conduction τ_T and convection τ_K. At $r = 1$ cm and $\lambda = 4.6$ W/(m K) ($T = 7 \times 10^3$ K), we have $\tau_T = c\rho r^2/\lambda \approx 1$ ms. The value of $\tau_K = \pi r/u \approx 10$ ms was obtained from the calculation of the period of rotation of gas in the arc column for vortex radius $r/2$ and velocity $u = 3$ m/s which corresponds to the experimental data. It follows from the assessment of characteristic times that further variation of the discharge structure will be largely defined by convection.

A calculation in a grid with twice larger space steps $h = 1$ mm and using the simplified model of volume radiation (11) was performed for the purpose of investigating the dynamics of arc formation with a longer duration of the process. The calculated temperature distribution and velocity field for the mean cross section of channel parallel to the electrode plane are given in Fig. 5 for time instant $t = 15$ ms. One can see in the figure that the vortex motion of gas during this time causes a significant deformation of the shape of discharge which assumes a meniscus shape in cross section. The maximal value of gas velocity within the arc column may be as high as 3.8 m/s. During the time of the process, the maximal value of temperature in the mean cross section first decreases from $T_{\max} = 7 \times 10^3$ K to $T_{\max} = 6.46 \times 10^3$ K by time instant $t \approx 10$ ms and then increases to $T_{\max} = 6.62 \times 10^3$ K ($t = 15$ ms). The overall voltage drop across the interelectrode gap was 93.5–95.5 V, with the electric field intensity of approximately 19 V/cm. In this calculation, the increase in the difference scale of the problem caused the decrease in the power transferred to the electrodes by the mechanism of heat conduction; therefore, the cross section of the arc spot is larger (12 mm^2) and the gas temperature in the zone of spreading is lower ($\approx 1.3 \times 10^4$ K).

The calculated value of maximal temperature $T_{\max}$ in the mean cross section of the discharge column corresponds to the measured value within 5%. In the electrode region, the model describes the process of thermal contraction of the arc; however, the calculated transverse dimension of the arc at the electrode exceeds significantly that of real microarcs. This is associated with the discrepancy between the difference step of numerical model and the characteristic spatial scale of the process in the vicinity of the electrodes. It is known [12] that the current density at the arc spot on the electrode is of the order of 10^4 A/cm^2 and higher; in so doing, the arc diameter at the electrode will not exceed 0.5 mm in the case of the current strength under consideration ($I \approx 20$ A). For calculating correctly the processes in the vicinity of the electrodes, the difference scale h in the numerical model must be much smaller than the characteristic dimensions of microarc; however, this will result in a corresponding increase in the required computer resources. A compromise solution may be reached, for example, by setting aside the layer in the vicinity of the electrodes as a separate computational domain with a reduced value of difference steps.

In selecting a model of radiation in the case of problems in radiation gas dynamics, it is necessary to allow for the optical thickness of the investigation object l, which may be determined by the value of absorption coefficient k_p averaged according to Planck and by the characteristic size of radiating region d. The use of

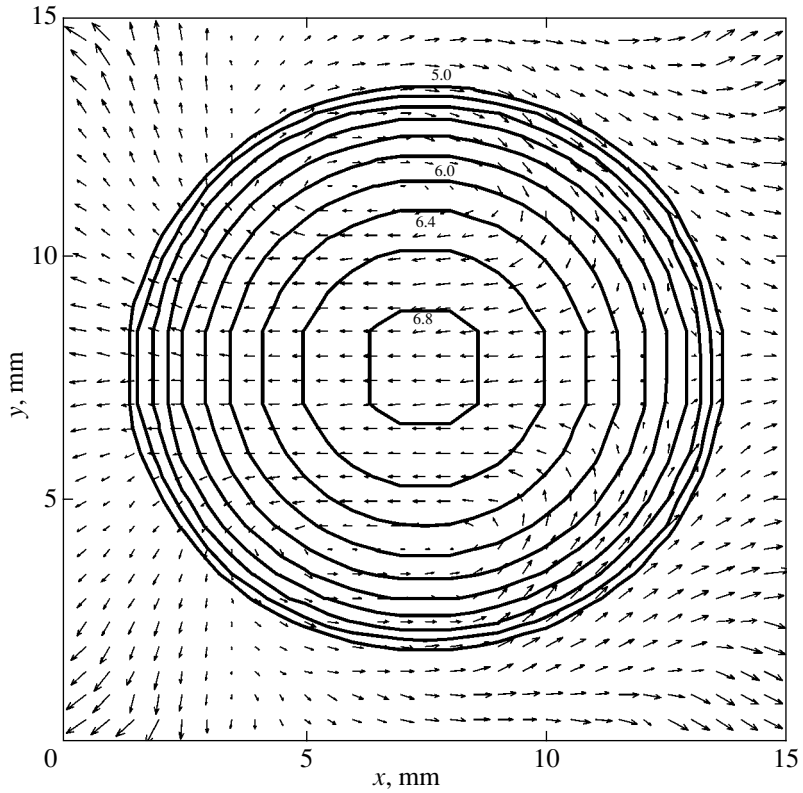

Fig. 4. The temperature distribution and the velocity field in the mean horizontal cross section of the channel for instant of time $t = 0.7$ ms, step $h = 0.5$ mm. The values of temperature on the isolines are in 10^3 K.

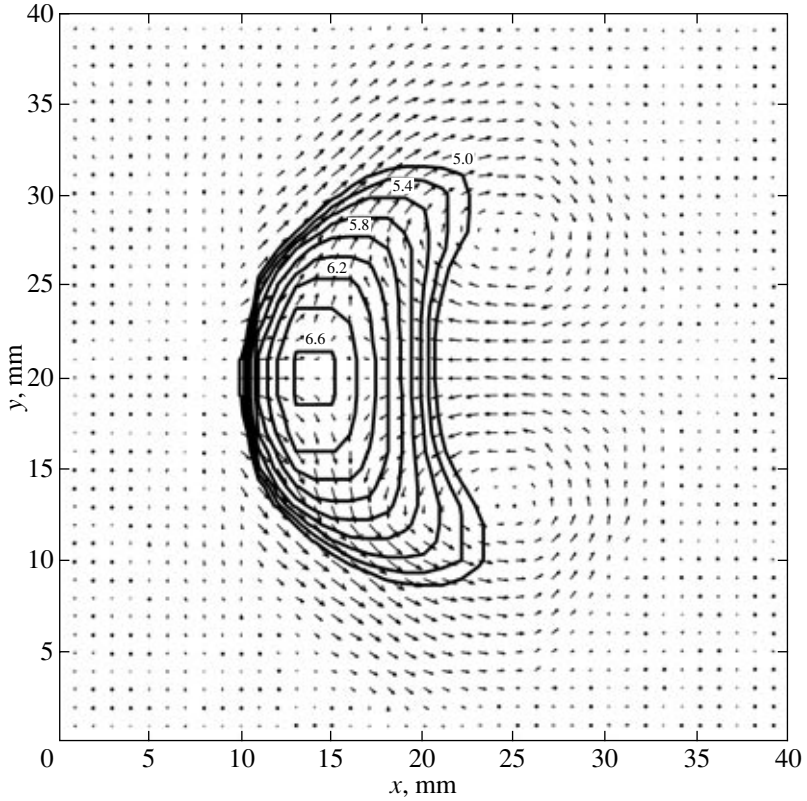

Fig. 5. The temperature distribution and the velocity field in the mean horizontal cross section of the channel for instant of time $t = 15$ ms, step $h = 1$ mm. The values of temperature on the isolines are in 10^3 K.

approximate formula (11) is quite justified in the case of calculation of energy loss in the discharge column in view of the small optical thickness of the latter, $l = dk_p \ll 1$, where $k_p = 0.0016$ cm^{-1} ($T = 7 \times 10^3$ K, $p = 10^5$ Pa) [10]. The values of temperature and absorption coefficient in the electrode region are higher, $k_p = 0.2$ cm^{-1} ($T = 1.4 \times 10^4$ K); the value of l here is likewise lower than unity but not to the extent of regarding the absorption processes as insignificant.

CONCLUSIONS

The results of comparison of calculation and experimental data lead one to conclude that the numerical model describes adequately the processes of heat transfer in electric-arc plasma which interacts with external magnetic field and transverse gas flow. The simulation made it possible to find the part played by various physical mechanisms in the formation of arc discharge column. The suggested numerical model is designed and most effective for the calculation of transient and highly nonuniform MGD flows; the calculation of the structure of slow and steady-state flows using this model calls for much computational effort.

REFERENCES

1. Zhainakov, A. and Urusov, R.M., *Teplofiz. Vys. Temp.*, 2002, vol. 40, no. 1, p. 13 (*High Temp.* (Engl. transl.), vol. 40, no. 1, p. 9).
2. Zhainakov, A., Urusov, R.M., and Urusova, T.E., *Teplofiz. Vys. Temp.*, 2002, vol. 40, no. 2, p. 199 (*High Temp.* (Engl. transl.), vol. 40, no. 2, p. 171).
3. Vasil'ev, E.N. and Nesterov, D.A., *Teplofiz. Vys. Temp.*, 2005, vol. 43, no. 3, p. 401 (*High Temp.* (Engl. transl.), vol. 43, no. 3, p. 396).
4. Vasil'ev, E.N. and Nesterov, D.A., *Zh. Prikl. Mekh. Tekh. Fiz.*, 2005, vol. 46, no. 6, p. 5.
5. Vasil'ev, E.N. and Nesterov, D.A., *Vychisl. Tekhnol.*, 2005, vol. 10, no. 6, p. 13.
6. Vasil'ev, E.N. and Nesterov, D.A., *Teplofiz. Vys. Temp.*, 2006, vol. 44, no. 3, p. 503 (*High Temp.* (Engl. transl.), vol. 44, no. 3).
7. Kukhtetskii, S.V., Lyubochko, V.A., Mikhailenko, L.P., and Pertsev, K.V., *Zh. Prikl. Mekh. Tekh. Fiz.*, 1986, no. 1, p. 40.
8. Sebald, N., *Appl. Phys.*, 1980, no. 21, p. 221.
9. Sokolova, I.A., *Mat. Model.*, 1997, vol. 9, no. 6, p. 113.
10. Avilova, I.V., Biberman, L.M., Vorob'ev, V.S., et al., *Opticheskie svoistva goryachego vozdukha* (Optical Properties of Hot Air), Moscow: Nauka, 1970.
11. Kamenshchikov, V.A., Plastinin, Yu.A., Nikolaev, V.M., and Novitskii, L.A., *Radiatsionnye svoistva gazov pri vysokikh temperaturakh* (Radiation Properties of Gases at High Temperatures), Moscow: Mashinostroenie, 1971.
12. Zhukov, M.F., Koroteev, A.S., and Uryukov, B.A., *Prikladnaya dinamika termicheskoi plazmy* (Applied Dynamics of Thermal Plasma), Novosibirsk: Nauka, 1975.